Molecular structure, optical and magnetic properties of metal-free phthalocyanine radical anions in crystalline salts (H2Pc˙−) (cryptand[2,2,2][Na+])·1.5C6H4Cl2 and (H2Pc˙−)(TOA+)·C...

ARTICLE *in* DALTON TRANSACTIONS · MARCH 2013

Impact Factor: 4.2 · DOI: 10.1039/c3dt50245g · Source: PubMed

Dalton Transactions

RSC Publishing

PAPER

Molecular structure, optical and magnetic properties of metal-free phthalocyanine radical anions in crystalline salts $(H_2Pc^{\bullet -})$(cryptand[2,2,2][Na^+])·1.5$C_6H_4Cl_2$ and $(H_2Pc^{\bullet -})(TOA^+)\cdot C_6H_4Cl_2$ (TOA^+ is tetraoctylammonium cation)†

Cite this: *Dalton Trans.*, 2013, **42**, 6810

Dmitri V. Konarev,*[a] Leokadiya V. Zorina,[b] Salavat S. Khasanov,[b] Aleksey L. Litvinov,[a] Akihiro Otsuka,[c] Hideki Yamochi,[c] Gunzi Saito[d] and Rimma N. Lyubovskaya[a]

Ionic compounds containing radical anions of metal-free phthalocyanine ($H_2Pc^{\bullet -}$): ($H_2Pc^{\bullet -}$)(cryptand[2,2,2][Na^+])·1.5$C_6H_4Cl_2$ (**1**) and ($H_2Pc^{\bullet -}$)(TOA^+)·$C_6H_4Cl_2$ (**2**) have been obtained as single crystals for the first time. Their crystal structures have been determined, and optical and magnetic properties have been investigated. The $H_2Pc^{\bullet -}$ radical anions have a slightly bowl-like shape with four pyrrole nitrogen atoms located below the molecular plane, while four phenylene substituents are located above this plane. Changes in the average length of N–C and C–C bonds in $H_2Pc^{\bullet -}$ in comparison with those in neutral H_2Pc indicate that negative charge is mainly delocalized over the 24-atom phthalocyanine ring rather than the phenylene substituents. The $H_2Pc^{\bullet -}$ formation is accompanied by a shift of up to 10 cm^{-1} and disappearance of some intense IR-active bands whereas the band of the N–H stretching mode is shifted by 21–27 cm^{-1} to larger wavenumbers. New bands attributed to $H_2Pc^{\bullet -}$ appear in the NIR spectra of the salts with maxima at 1033 and 1028 nm for **1** and **2**, respectively. The formation of $H_2Pc^{\bullet -}$ is accompanied by the splitting of the Soret and Q-bands of H_2Pc into several bands and their blue-shift up to 32 nm. Narrow EPR signals with g = 2.0033 and linewidth of 0.16–0.24 mT at room temperature in the spectra of the salts were attributed to the $H_2Pc^{\bullet -}$ radical anions. According to SQUID measurements they have S = 1/2 spin states with effective magnetic moments of 1.73 (**1**) and 1.78 (**2**) μ_B at 300 K. Magnetic behavior of **1** and **2** follows the Curie–Weiss law with negative Weiss temperatures of −0.9 and −0.5 K, respectively, indicating weak antiferromagnetic interactions of spins. The EPR signal splits into two lines below 120 and 80 K for **1** and **2**, respectively and these lines are noticeably broadened below 25 K.

Received 24th January 2013,
Accepted 15th February 2013

DOI: 10.1039/c3dt50245g

www.rsc.org/dalton

Introduction

Metal-free and metal-containing phthalocyanines are promising components in the design of optical, conducting and magnetic materials.[1–6] Up to now functional phthalocyanine compounds were obtained mainly by oxidation. For example, a series of molecular metals was synthesized by iodine or electrochemical oxidation of MPc (M = H_2, Ni(II), Cu(II)).[3,5] Highly conducting materials were prepared by the electrochemical oxidation of the $[M(III)Pc(2-)(CN)_2]^-$ anions in the presence of organic cations.[4,5]

Anionic phthalocyanines can also show promising conducting and magnetic properties.[7,8] However, although phthalocyanine anions are chemically and electrochemically available, they are scarcely characterized in the solid state and only the data in solution are known on these anions.[9,10] One of the reasons for this is their high air sensitivity. Indeed, phthalocyanine anions can be easily oxidized by oxygen due to their negative reduction potentials ($E^{0/-}$ of H_2Pc, Ni(II)Pc(2−), Zn(II)Pc(2−) is equal to −0.59 to −0.78 V *vs.* SCE in non-coordinating 1-methylnaphthalene at 150 °C).[11] At present, anionic metal phthalocyanines are mainly obtained in the solid state by doping with alkali metals in gas phase.[12,13] In crystalline form

[a]*Institute of Problems of Chemical Physics RAS, Chernogolovka, Moscow region, 142432 Russia. E-mail: konarev@icp.ac.ru*
[b]*Institute of Solid State Physics RAS, Chernogolovka, Moscow region, 142432 Russia*
[c]*Research Center for Low Temperature and Materials Sciences, Kyoto University, Kyoto 606-8501, Japan*
[d]*Faculty of Agriculture, Meijo University, 1-501 Shiogamaguchi, Tempaku-ku, Nagoya 468-8502, Japan*

†Electronic supplementary information (ESI) available: IR-spectra of **1**, **2** and starting compounds and EPR data for compound **2**. CCDC 919370 and 919371 for **1** and **2**, respectively. For ESI and crystallographic data in CIF or other electronic format see DOI: 10.1039/c3dt50245g

one compound with cobalt(I) and several compounds with iron(I) phthalocyanine anions were obtained and their optical and magnetic properties were studied.[14–17]

Reduction of metal-free phthalocyanine (H_2Pc) yields the $H_2Pc^{\cdot -}$ radical anion. Though electrochemistry of H_2Pc is studied up to the formation of tetraanion in solution,[18] no compounds containing these radical anions have been obtained and characterized in the solid state up to now. Nevertheless, the information on the properties of $H_2Pc^{\cdot -}$ in the solid state is very important for both developing new functional materials based on metal-free phthalocyanine and understanding the properties of compounds containing anions of metal phthalocyanines. At the formation of these anions an electron can transfer to the metal center to form the $[M(I)Pc(2-)]^-$ anions (Co(II)Pc(2−) and Fe(II)Pc(2−)) or the phthalocyanine ring can accept an electron to form the $[M(II)Pc(3-)]^-$ anions (Zn(II)Pc(2−), Ni(II)Pc(2−) and Cu(II)Pc(2−)).[10] Some intermediate states with electron transfer from the M(I) center to the phthalocyanine ring are also possible. For example, coordination of electron donating ligands like dimethyl sulfoxide to the $[Fe(I)Pc(2-)]^-$ anions manifests new EPR signal attributed to the $[M(II)Pc(3-)]^-$ species.[19] Recently we found that the formation of coordination $\{[Fe(I)Pc(2-)]^-\}_2$ dimers in ternary ionic complexes, in which the nitrogen atom of one phthalocyanine anion weakly coordinates to the iron(I) atom of neighboring $[Fe(I)Pc(2-)]^-$ anion, also results in narrow EPR signals with a *g*-factor close to free-electron value (2.0023) due to the appearance of the $[M(II)Pc(3-)]^-$ species.[17]

In this work we obtained for the first time the salts containing radical anions of metal-free phthalocyanine ($H_2Pc^{\cdot -}$) as single crystals. Crystal structures, optical and magnetic properties of $(H_2Pc^{\cdot -})(cryptand[2,2,2][Na^+])\cdot 1.5C_6H_4Cl_2$ (**1**) and $(H_2Pc^{\cdot -})(TOA^+)\cdot C_6H_4Cl_2$ (**2**) were studied in the solid state. We discuss the molecular structure of the $H_2Pc^{\cdot -}$ radical anions, changes in the IR- and UV-visible-NIR spectra at the formation of $H_2Pc^{\cdot -}$, electronic state of $H_2Pc^{\cdot -}$ and magnetic interactions in solid salts **1** and **2**.

Results and discussion

a. Synthesis

We showed that sodium fluorenone is suitable reductant for selective generation of fullerene C_{60}^{2-} dianions in *o*-dichlorobenzene ($C_6H_4Cl_2$) solution in the presence of different organic cations.[20] Since reduction potentials of phthalocyanines[10,11] are shifted to negative values relatively to those of fullerenes,[21] sodium fluorenone selectively generates phthalocyanine monoanions only in these conditions even in an excess of reductant. Several compounds containing $[Fe(I)Pc(2-)]^-$ anions were obtained by this method and characterized in the solid state.[16] Metal-free phthalocyanine H_2Pc completely dissolves within 5 minutes at the reduction by sodium fluorenone in the presence of cryptand[2,2,2] or tetraoctylammonium bromide (TOA^+Br^-) in $C_6H_4Cl_2$ and deep blue solution of $H_2Pc^{\cdot -}$ forms. Slow diffusion of hexane into the obtained solutions within 1.5–2 months allows one to obtain crystals of $(H_2Pc^{\cdot -})(cryptand[2,2,2][Na^+])\cdot 1.5C_6H_4Cl_2$ (**1**) and $(H_2Pc^{\cdot -})(TOA^+)\cdot C_6H_4Cl_2$ (**2**). Composition of the salts was determined from X-ray diffraction on single crystals. Several crystals tested from the synthesis had the same unit cell parameters which indicated the formation of a single phase in the syntheses of **1** and **2**.

b. Optical properties of 1 and 2

IR-spectra of the starting H_2Pc and salts **1** and **2** measured in KBr pellets are shown in Fig. 1. The position of absorption bands in these spectra are listed in the ESI.† Nearly all absorption bands observed in the spectrum of H_2Pc are reproduced in the spectra of **1** and **2**. However, noticeable shifts and changes in intensity of some strong absorption bands are observed. For example, the strong band at 717 cm^{-1} is shifted by 8–10 cm^{-1} in the spectra of the salts to smaller wavenumbers, the band at 751 cm^{-1} of middle intensity is shifted by 10 cm^{-1} to larger wavenumbers and strongly increases in intensity, and the strong bands of H_2Pc at 1004 and 1118 cm^{-1} are nearly absent. There are also noticeable changes in the

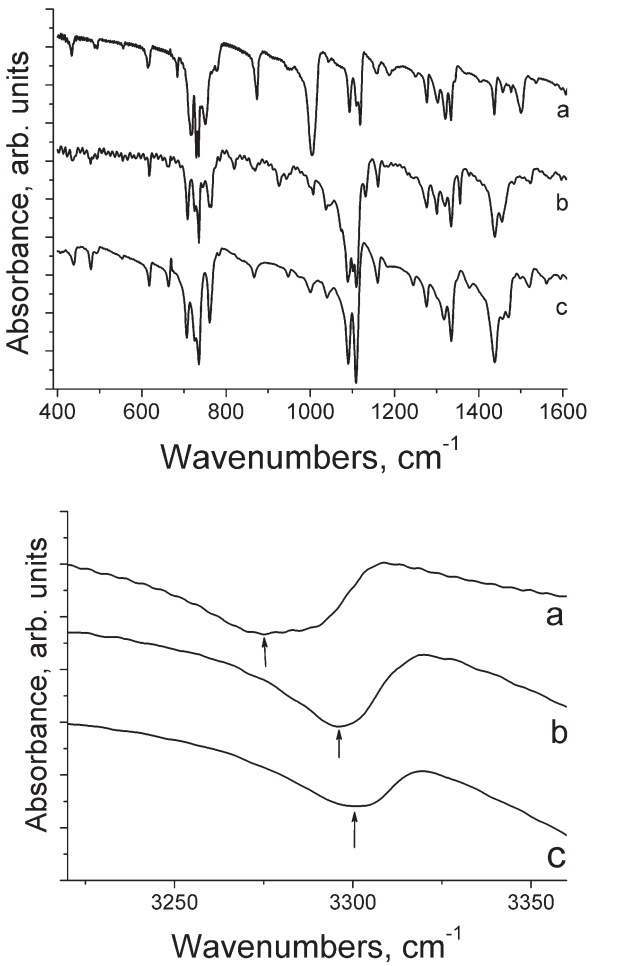

Fig. 1 IR-spectra of starting H_2Pc (a), salts **1** (b) and **2** (c) in the 400–1600 (top panel) and 3200–3350 cm^{-1} (bottom panel) regions. Spectra of **1** and **2** were measured in an anaerobic condition.

positions of some absorption bands of weak and middle intensity (see ESI†).

Metal-free phthalocyanine has two hydrogen atoms bonded to pyrrole nitrogen atoms. The position of the band corresponding to the vibration of the N–H bonds in the spectrum of starting H_2Pc is at 3274 cm^{-1} (Fig. 1b). This band is noticeably shifted in the spectra of **1** and **2** having positions at 3295 and 3301 cm^{-1}, respectively (the shift to larger wavenumbers is 21–27 cm^{-1}). The position of absorption bands corresponding to the C–H vibrations in the phenylene substituents of H_2Pc at 3000–3080 cm^{-1} remains nearly unchanged in the spectra of the salts. Therefore, the formation of $H_2Pc^{\cdot -}$ strongly affects the length of the N–H bonds. On the whole, we can conclude that noticeable redistribution of bond lengths is realized in the ionization of neutral H_2Pc to the $H_2Pc^{\cdot -}$ radical anion.

Spectra of the starting H_2Pc and salts **1** and **2** in the UV-visible-NIR region are shown in Fig. 2. There are many absorption bands in the spectra of the salts all of which can be unambiguously attributed to the $H_2Pc^{\cdot -}$ radical anions. The Soret band is observed in the spectrum of H_2Pc as one broad band with the maximum at 339 nm. The Soret band of $H_2Pc^{\cdot -}$ in the spectra of the salts is essentially better resolved and consists of three bands with maxima at 269, 329, and 389 nm (**1**) and 269, 327, and 389 nm (**2**) (Fig. 2). Q-bands observed in the visible spectrum of H_2Pc are split into two bands at 636 and 703 nm. The formation of $H_2Pc^{\cdot -}$ produces three or four well resolved Q-bands with maxima at 591, 641, and 671 nm (**1**) and 583, 621, 646, and 676 nm (**2**) (Fig. 2). It is seen that lower-energy Q-bands are blue-shifted up to 32 nm and are essentially narrower as compared with those in the spectrum of H_2Pc. The latter fact indicates isolation of $H_2Pc^{\cdot -}$ both in **1** and **2**. A noticeable difference in the spectra of neutral and negatively charged H_2Pc is observed in the NIR range. Neutral H_2Pc has no absorption in this range but the $H_2Pc^{\cdot -}$ radical anions manifest intense absorption up to 1200 nm with maxima at 838, 935, and 1033 nm (**1**) and 818, 858, 930, 968, and 1028 nm (**2**) (Fig. 2). Thus, the appearance of bands in the NIR range can be the evidence of the formation of the $H_2Pc^{\cdot -}$ radical anions.

c. Crystal structures of 1 and 2 and molecular structure of $H_2Pc^{\cdot -}$ in solid state

Both salts **1** and **2** have monoclinic lattices with well-ordered components: one each of $H_2Pc^{\cdot -}$, the cryptand[2,2,2]·[Na^+] cation is crystallographically independent along with one and a half solvent $C_6H_4Cl_2$ molecules in **1**, and two of each $H_2Pc^{\cdot -}$, the TOA^+ cations and solvent $C_6H_4Cl_2$ molecules are unique in **2**. Solvent molecules in one position are disordered in both salts between two orientations. A pair of hydrogen atoms in the $H_2Pc^{\cdot -}$ anion bound to pyrrole nitrogen atoms is disordered in salt **1** over two positions with a 0.56 : 0.44 occupancy ratio. The crystal structure of **1** was solved with good precision allowing the bond lengths in $H_2Pc^{\cdot -}$ to be analysed, whereas for crystal structure of **2** we can discuss only general packing due to high *R*-factor value (R_1 = 0.0988) resulting from the weak diffraction ability of the crystal **2** at high θ angles. Mean intensity of reflections at resolution below 1 Å ($\theta > 20°$ for MoK_α) is less than $2\sigma(I)$ criterion.

The crystal structure of **1** contains channels arranged along the *a* axis and formed by four $H_2Pc^{\cdot -}$ planes (Fig. 3). The channels are occupied by double chains of alternating cryptand[2,2,2]·[Na^+] cations and solvent $C_6H_4Cl_2$ molecules. The size of the channels is defined by distances between phthalocyanine planes (11.74 × 19.05 $Å^2$). The cryptand[2,2,2]·[Na^+] cations form van der Waals contacts mainly with $H_2Pc^{\cdot -}$, where the H(cryptand[2,2,2]·[Na^+])···C,N($H_2Pc^{\cdot -}$) contacts are in the 2.66–2.86 Å range. A previously studied salt with iron(I) phthalocyanine anions [($Fe^{I}Pc(2-)^-$]·(cryptand[2,2,2]·[Na^+])·$C_6H_4Cl_2$ has similar channels formed by four phthalocyanine planes.[16] However, their arrangement in this salt is different from that in **1**. All channels in the salt with [$Fe^{I}Pc(2-)$]$^-$ are identical, whereas there are two types of channel arrangement

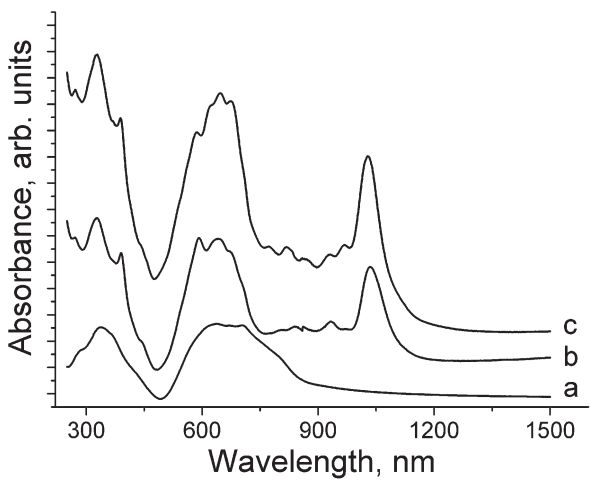

Fig. 2 Spectra of H_2Pc (a); salts **1** (b) and **2** (c) in the UV-visible-NIR range in KBr pellets measured in an anaerobic condition for **1** and **2**.

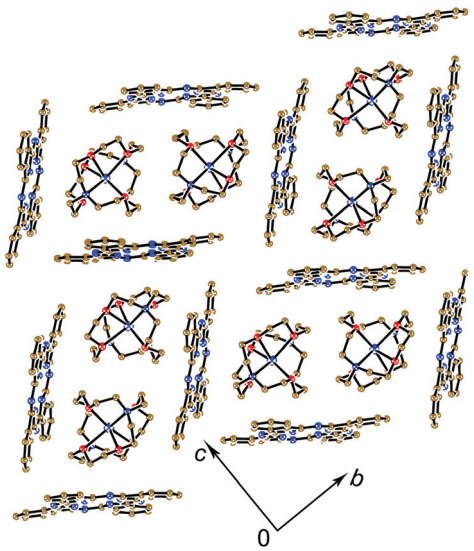

Fig. 3 Crystal structure of **1** viewed along the *a* axis.

in **1** which are coincident at the 180° rotation around the screw axis arranged parallel to the crystallographic *a* axis (Fig. 3).

The using of bulky TOA^+ cations provides different structural packing of **2**. Two TOA^+ cations and two solvent $C_6H_4Cl_2$ molecules are sandwiched between two phthalocyanine planes (Fig. 4a). These structural blocks have two orientations which alternate along the [110], [1$\bar{1}$0] and [001] directions (Fig. 4b). As a result, every block is surrounded by six blocks of the other orientation. The TOA^+ cations form van der Waals contacts also mainly with $H_2Pc^{\cdot -}$, where the $H(TOA^+)\cdots C$, $N(H_2Pc^{\cdot -})$ contacts are in the 2.77–2.89 Å range.

Geometry of the $H_2Pc^{\cdot -}$ radical anion was studied in **1**. This anion has a slightly bowl-like shape with all four pyrrole nitrogen atoms located below the molecular phthalocyanine plane, while four phenylene substituents are located above this plane (Fig. 5b, Table 1). This leads to molecular symmetry C_1 opposite to the D_{2h} symmetry supposed for the free molecule. It should be noted that neutral H_2Pc has a different distortion of the macrocycle. It is slightly distorted at the corners and two of four phenylene substituents (adjacent to each other) are located below the phthalocyanine plane, while the other two are above this plane according to the inversion symmetry of the molecule.[22] Deviation of atoms from the molecular plane of the neutral phthalocyanine does not exceed ±0.055 Å, *i.e.* H_2Pc is more flattened in comparison with $H_2Pc^{\cdot -}$ (Table 1). Averaged bond lengths in the structures of neutral H_2Pc and the $H_2Pc^{\cdot -}$ radical anions in **1** are listed in Table 1. The difference in the bond lengths in neutral and negatively charged H_2Pc is relatively small and does not exceed 0.01 Å. Nevertheless, it is seen as a common tendency in $H_2Pc^{\cdot -}$ to change the bond lengths involved in the inner 24-atom phthalocyanine plane. The C–C bond lengths of the phenylene substituents do not change. These data indicate that negative charge is delocalized over the 24-atom phthalocyanine ring in accordance with the data from IR-spectra. The strongest shift in the IR-spectra at the reduction of H_2Pc is observed for the absorption bands corresponding to the vibrations of the N–H bonds with pyrrole nitrogen atoms, whereas the absorption bands corresponding to the vibration of the C–H bonds with carbon atoms of phenylene substituents remain nearly unchanged. The averaged lengths of the C–N bonds with pyrrole nitrogen atoms are shortened by 0.009 Å, whereas those for the imine nitrogen atoms are elongated by 0.008 Å. Therefore, the lengths of both types of the C–N bonds become closer to each other. We can conclude that negative charge on H_2Pc tends to equalize the C–N bonds with pyrrole and imine nitrogen atoms and that results in slightly bowl-like shape distortion of the phthalocyanine macrocycle.

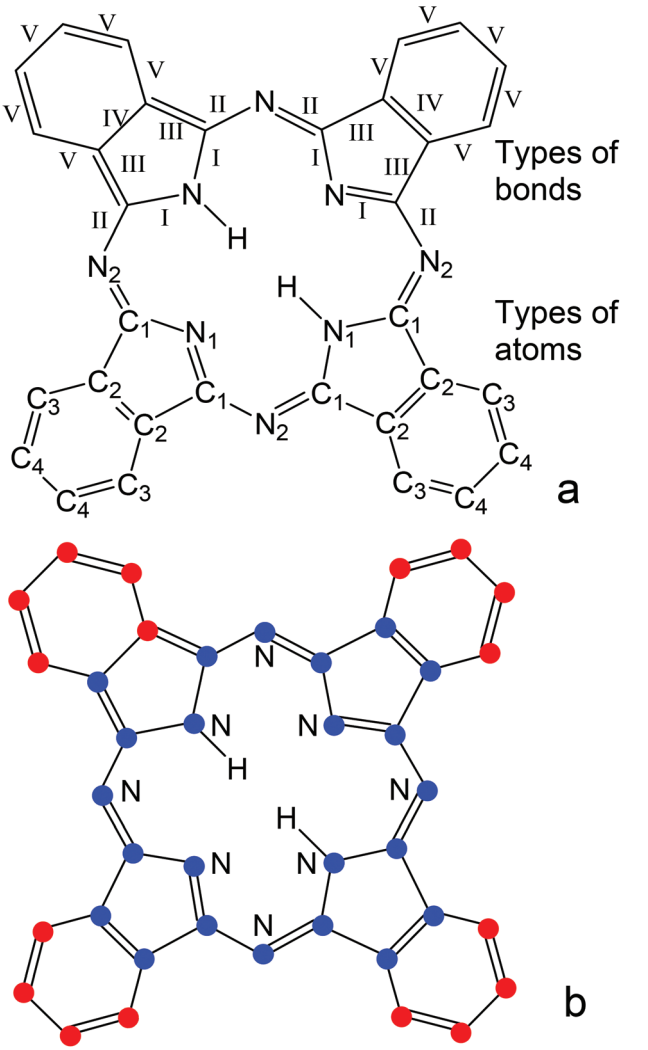

Fig. 5 (a) Types of bonds and atoms in phthalocyanine molecule; (b) distortion of phthalocyanine macrocycle (red and blue points show atoms located above and below the phthalocyanine molecular plane, respectively).

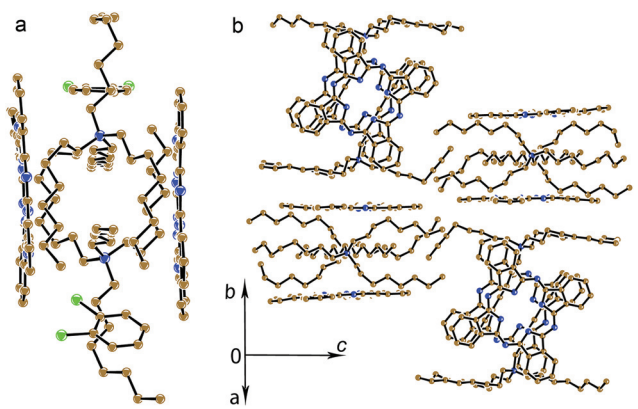

Fig. 4 (a) View of main structural block of **2** containing the TOA^+ cations and solvent $C_6H_4Cl_2$ molecules sandwiched between two phthalocyanine planes; (b) the arrangement of these structural blocks in the unit cell of **2**.

d. Magnetic properties of 1 and 2

The magnetic properties of **1** and **2** were studied by SQUID and EPR techniques. According to SQUID measurements, the effective magnetic moments of **1** and **2** are equal to 1.73 and 1.78 μ_B at 300 K. Since both cryptand[2,2,2][Na^+] and TOA^+

Table 1 Averaged bond lengths and deviation of atoms from the phthalocyanine molecular plane in the structures of neutral H_2Pc and $H_2Pc^{\cdot -}$ in **1**. Type of bonds and number of atoms are shown in Fig. 5

Type of bond	Neutral H_2Pc[a] (Å)[22]	$H_2Pc^{\cdot -}$ in **1**[a] (Å)	Difference (Å)
C–N bonds of type I (8 bonds)	1.372(4)	1.363(9)	−0.009
C–N bonds of type II (8 bonds)	1.327(2)	1.335(4)	+0.008
C–C bonds of type III (8 bonds)	1.456(5)	1.463(8)	+0.007
C–C bonds of type IV (4 bonds)	1.397(3)	1.397(5)	0
C–C bonds of type V (20 bonds)	1.388(6)	1.391(6)	+0.003
Number of atoms			
N_1 atoms (4 atoms)	—	+0.082	
N_2 atoms (4 atoms)	—	+0.063	
C_1 atoms (8 atoms)	—	+0.067	
C_2 atoms (8 atoms)	—	+0.016	
C_3 atoms (8 atoms)	—	−0.045	
C_4 atoms (8 atoms)	—	−0.123	

[a] Standard deviation of mean bond lengths is given in brackets. Accuracy for individual bond lengths is noticeably lower (0.002 Å for H_2Pc and 0.003 Å for $H_2Pc^{\cdot -}$).

cations are diamagnetic, we can conclude that the $H_2Pc^{\cdot -}$ radical anions have $S = 1/2$ spin state (the calculated magnetic moment for the system with one non-interacting $S = 1/2$ spin is 1.73 μ_B). Magnetic behavior of **1** and **2** is described by the Curie–Weiss law in the 10–300 K region with negative Weiss temperatures of −0.9 and −0.5 K, respectively, indicating weak antiferromagnetic interactions of spins in these salts. Weak magnetic interaction is a result of relatively large distances between $H_2Pc^{\cdot -}$ in the structures of **1** and **2** which are separated by bulky cations and solvent molecules.

Data of EPR measurements for **1** are given in Fig. 6 and those for **2** are presented in ESI.† The EPR spectra of both salts show intense narrow signals with $g = 2.0033$ and linewidth (ΔH) of 0.16–0.24 mT at room temperature attributed to $H_2Pc^{\cdot -}$ (Fig. 6a for **1**). The g-factor and ΔH of the signals remain unchanged down to 120 and 80 K, respectively for **1** (Fig. 6b and c) and **2**. Below these temperatures the splitting of the EPR signal into two lines is observed and these lines are shifted to higher and lower g-factors with the temperature decrease and noticeably broadened below 25 K (Fig. 6c for **1**). Since both salts manifest weak antiferromagnetic interaction of spins, the observed shift and broadening of the lines can be attributed to antiferromagnetic interaction of spins localized on $H_2Pc^{\cdot -}$. It was shown that in ionic C_{60} complexes and salts with weak antiferromagnetic interaction of spins generally the splitting of EPR signal into two lines is observed, and these lines are shifted in the opposite directions and broadened at low temperatures.[23–26]

Conclusion

We obtained ionic compounds **1** and **2** containing radical anions of metal-free phthalocyanine ($H_2Pc^{\cdot -}$). It was found that negative charge delocalized over the 24-atom phthalocyanine ring equalizes the C–N bonds with pyrrole and imine nitrogen atoms and provides slightly bowl-like shape of phthalocyanine macrocycle. Charging of H_2Pc affects the position and intensity of some absorption bands in its IR-spectrum, and new intense bands appear in the NIR-spectra of the salts. The narrow EPR signal with $g = 2.0033$ and linewidth of 0.16–0.24 mT was attributed to $H_2Pc^{\cdot -}$. According to SQUID measurements it has an $S = 1/2$ spin state with effective magnetic moments close to 1.73 μ_B. Spins localized on $H_2Pc^{\cdot -}$ interact weakly antiferromagnetically and that provides the splitting of the EPR signal into two lines at low temperatures. The obtained data are useful to identify the $H_2Pc^{\cdot -}$ radical anions in the complexes and salts of metal-free phthalocyanines and establish the formation of the $[M(II)Pc(3-)]^-$ species in the anions of metal-containing phthalocyanines.

Experimental

Materials

Metal-free phthalocyanine (H_2Pc), cryptand[2,2,2] and (TOA^+)(Br^-) were purchased from Aldrich. Sodium fluorenone was obtained as previously described.[27] Solvents were purified in argon atmosphere. *o*-Dichlorobenzene ($C_6H_4Cl_2$) was distilled over CaH_2 under reduced pressure and hexane was distilled over Na/benzophenone. The solvents were degassed and stored in a glove box. All manipulations for the synthesis of air-

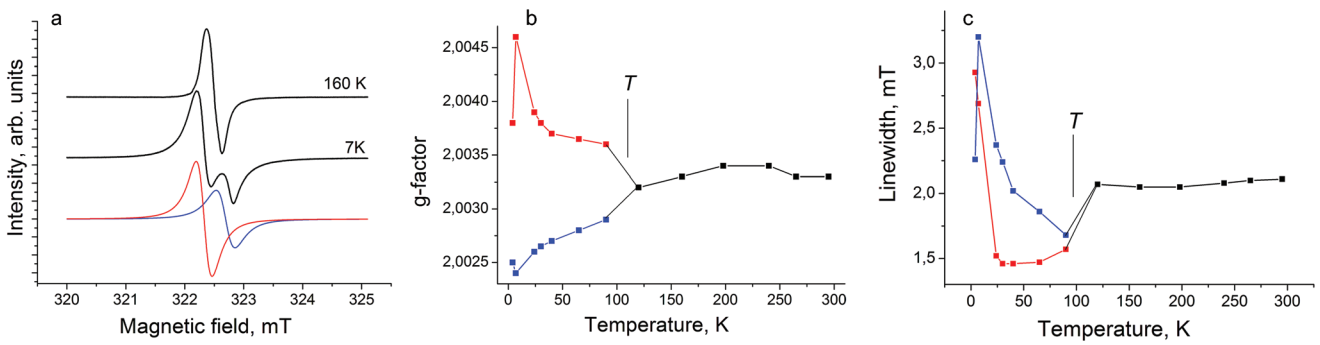

Fig. 6 (a) EPR spectrum of **1** at 160 and 7 K. The fitting of the signal by two Lorentzian lines for spectrum at 7 K is shown below; Temperature dependence of g-factor (b) and linewidth (c) of EPR signal in **1**. "T" marks the temperature of splitting of the EPR signal into two lines.

sensitive **1** and **2** were carried out in a MBraun 150B-G glove box with controlled atmosphere (O_2, H_2O < 1 ppm). The crystals were stored in the glove box and sealed in 2 mm quartz tubes for EPR and SQUID measurements under 10^{-3} Torr. KBr pellets for IR- and UV-visible-NIR measurements were prepared in the glove box.

Synthesis

Reduction of H_2Pc (21.8 mg, 0.042 mmol) by slight excess of sodium fluorenone (11 mg, 0.054 mmol) in the presence of stoichiometric amount of cryptand[2,2,2] (15.8 mg, 0.042 mmol) upon stirring in 15 mL of *o*-dichlorobenzene at 60 °C for 4 hours produced a deep blue solution of the $H_2Pc^{\cdot -}$ salt with sodium cryptand cations. The solution was cooled and filtered into a 50 mL glass tube 1.8 cm in diameter with a ground glass plug. 25 mL of hexane was layered over the obtained solution. Slow diffusion of hexane into the obtained solution during 6 weeks yielded the crystals of $(H_2Pc^{\cdot -})$-(cryptand[2,2,2][Na^+])·$1.5C_6H_4Cl_2$ (**1**) on the walls of the tube. The solvent was decanted from the crystals which were then washed with hexane (yield 65%). The crystals were black rhombic plates up to 1 × 0.6 × 0.2 mm^3 in size with characteristic copper luster. The composition of **1** was determined by X-ray structural analysis on a single crystal. Several crystals tested from the synthesis had the same unit cell parameters.

Reduction of H_2Pc (21.8 mg, 0.042 mmol) by slight excess of sodium fluorenone (11 mg, 0.054 mmol) in the presence of stoichiometric amount of TOA^+Br^- (23 mg, 0.042 mmol) upon stirring in 16 mL of *o*-dichlorobenzene at 60 °C for 4 hours produced deep blue solution. The solution was cooled and filtered into a 50 mL glass tube 1.8 cm in diameter with a ground glass plug. 25 mL of hexane was layered over the obtained solution. Slow diffusion of hexane into the obtained solution during 8 weeks yielded the crystals of $(H_2Pc^{\cdot -})$ (TOA^+)·$C_6H_4Cl_2$ (**2**) on the walls of the tube. The solvent was decanted from the crystals which were then washed with hexane (yield 32%). The crystals were black rhombic plates up to 1 × 0.6 × 0.2 mm^3 in size with characteristic copper luster. The composition of **2** was determined by X-ray structural analysis on a single crystal. Several crystals tested from the synthesis had the same unit cell parameters.

General

UV-visible-NIR spectra were measured in KBr pellets on a Perkin Elmer Lambda 1050 spectrometer in the 250–2500 nm range. FT-IR spectra were measured in KBr pellets with a Perkin-Elmer Spectrum 400 spectrometer (400–7800 cm^{-1}). EPR spectra were recorded from 293 down to 4 K with a JEOL JES-TE 200 X-band ESR spectrometer. A Quantum Design MPMS-XL SQUID magnetometer was used to measure static magnetic susceptibility (χ_M) of **1** and **2** at 100 mT magnetic field in cooling and heating conditions from 300 down to 1.9 K and back from 1.9 up to 300 K. Temperature independent core diamagnetic susceptibility (χ_0) was estimated in the 10–300 K range by the extrapolation of the data in the high-temperature range. A sample holder contribution and χ_0 were subtracted from the experimental values. An effective magnetic moment (μ_{eff}) was calculated with an appropriate formula: $\mu_{eff} = (8\chi_M T)^{1/2}$.

X-ray crystal structure determination

Crystal data for 1 at 120(1) K. $C_{59}H_{60}Cl_3N_{10}NaO_6$, M_r = 1134.51 g mol^{-1}, black plate, monoclinic, $P2_1/n$, a = 12.5237(6) Å, b = 24.7015(14) Å, c = 17.8755(10) Å, β = 95.685(5)°, V = 5502.7(5) $Å^3$, Z = 4, d_{calc} = 1.369 g cm^{-3}, μ = 0.237 mm^{-1}, $F(000)$ = 2376, $2\theta_{max}$ = 53.46°, reflections measured 46 209, unique reflections 11 651, reflections with $I > 2\sigma(I)$ = 9067, R_{int} = 0.054, parameters refined 798, restraints 211, R_1 = 0.0512, wR_2 = 0.1213, G.O.F. = 1.002.

Crystal data for 2 at 130(1) K. $C_{70}H_{90}Cl_2N_9$, M_r = 1128.41 g mol^{-1}, black rhomb, monoclinic, $P2_1/c$, a = 16.1492(11) Å, b = 23.9690(15) Å, c = 32.223(2) Å, β = 90.537(7)°, V = 12 472.3(15) $Å^3$, Z = 8, d_{calc} = 1.202 g cm^{-3}, μ = 0.154 mm^{-1}, $F(000)$ = 4856, $2\theta_{max}$ = 54.2°, reflections measured 73 448, unique reflections 25 719, reflections with $I > 2\sigma(I)$ = 13 955, R_{int} = 0.065, parameters refined 1516, restraints 192, R_1 = 0.0988, wR_2 = 0.2983, G.O.F. = 1.054.

X-ray diffraction data for **1** and **2** were collected on an Oxford diffraction "Gemini-R" CCD diffractometer with graphite monochromated MoK_α radiation using an Oxford Instrument Cryojet system. Raw data reduction to F^2 was carried out using CrysAlisPro, Oxford Diffraction Ltd. The structures were solved by direct method and refined by the full-matrix least-squares method against F^2 using SHELX-97.[28] Non-hydrogen atoms were refined in the anisotropic approximation. Positions of hydrogen atoms connected to pyrrole nitrogen atoms of $H_2Pc^{\cdot -}$ were found in difference electron density map. This pair of H-atoms appeared to be ordered in the structure **2** and disordered over two sites with occupancy ratio of 0.56 : 0.44 in the structure **1**. Other hydrogen atoms were positioned geometrically. Subsequently, all the H atoms were refined by the "riding" model with $U_{iso} = 1.2U_{eq}$ of the connected non-hydrogen atom or as ideal CH_3 groups with $U_{iso} = 1.5U_{eq}$. For crystallographic data in CIF or other electronic format see the ESI.†

Acknowledgements

The work was supported by RFBR grant No. 13-03-00769 and 12-03-92017 (Japan–Russia Research Cooperative Program), Grant-in-Aid Scientific Research from JSPS, Japan (23225005) and MEXT, Japan (20110006).

Notes and references

1 T. Nyokong, *Coord. Chem. Rev.*, 2007, **251**, 1707.
2 C. G. Claessens, W. J. Blau, M. Cook, M. Hanack, R. J. M. Nolte, T. Torres and D. Wöhrle, *Monatsh. Chem.*, 2001, **132**, 3.

3 C. S. Schramm, R. P. Scaringe, D. R. Stojakovic, B. M. Hoffman, J. A. Ibbers and T. J. Marks, *J. Am. Chem. Soc.*, 1980, **102**, 6702.
4 H. Hasegawa, T. Naito, T. Inabe, T. Akutagawa and T. Nakamura, *J. Mater. Chem.*, 1998, **8**, 1567.
5 T. Inabe and H. Tajima, *Chem. Rev.*, 2004, **104**, 5503.
6 D. K. Rittenberg, L. Baars-Hibbe, A. B. Böhm and J. S. Miller, *J. Mater. Chem.*, 2000, **10**, 241.
7 E. Tosatti, M. Fabrizio, J. Tóbik and G. E. Santoro, *Phys. Rev. Lett.*, 2004, **93**, 117002.
8 D. V. Konarev, L. V. Zorina, S. S. Khasanov, E. U. Hakimova and R. N. Lyubovskaya, *New J. Chem.*, 2012, **36**, 48.
9 R. Taube, *Pure Appl. Chem.*, 1974, **38**, 427.
10 A. B. P. Lever, E. P. Milaeva and G. Speier, in *Phthalocyanines, properties and applications*, ed. C. C. Lezuoff and A. B. P. Lever, VCH, New York, 1993, vol. 3, pp. 1–70.
11 R. H. Campbell, G. A. Heath, G. T. Hefter and R. C. S. McQueen, *J. Chem. Soc., Chem. Commun.*, 1983, 1123.
12 S. Margadonna, K. Prassides, Y. Iwasa, Y. Taguchi, M. F. Craciun, S. Rogge and A. F. Morpurgo, *Inorg. Chem.*, 2006, **45**, 10472.
13 Y. Taguchi, T. Miyake, S. Margadonna, K. Kato, K. Prassides and Y. Iwasa, *J. Am. Chem. Soc.*, 2006, **128**, 3313.
14 H. Huckstadt and H. Homborg, *Z. Anorg. Allg. Chem.*, 1998, **624**, 715.
15 M. Tahiri, P. Doppelt, J. Fischer and R. Weiss, *Inorg. Chim. Acta*, 1987, **127**, L1.
16 D. V. Konarev, A. V. Kuzmin, S. V. Simonov, S. S. Khasanov, A. Otsuka, H. Yamochi, G. Saito and R. N. Lyubovskaya, *Dalton Trans.*, 2012, **41**, 13841.
17 D. V. Konarev, M. Ishikawa, S. S. Khasanov, A. Otsuka, H. Yamochi, G. Saito and R. N. Lyubovskaya, *Inorg. Chem.*, DOI: 10.1021/ic3025364, in press.
18 D. W. Clack, N. S. Hush and I. S. Woolsey, *Inorg. Chim. Acta*, 1976, **19**, 129.
19 A. B. P. Lever and J. P. Wilshire, *Inorg. Chem.*, 1978, **17**, 1145.
20 D. V. Konarev, A. V. Kuzmin, S. V. Simonov, S. S. Khasanov, E. I. Yudanova, G. Saito and R. N. Lyubovskaya, *Phys. Chem. Chem. Phys.*, 2013, submitted.
21 Q. Xie, E. Perez-Cordero and L. Echegoyen, *J. Am. Chem. Soc.*, 1992, **114**, 3977.
22 S. Matsumoto, K. Matsuhama and J. Mizuguchi, *Acta Crystallogr., Sect. C: Cryst. Struct. Commun.*, 1999, **55**, 131.
23 D. V. Konarev, A.Yu. Kovalevsky, S. S. Khasanov, G. Saito, A. Otsuka and R. N. Lyubovskaya, *Eur. J. Inorg. Chem.*, 2005, 4822.
24 D. V. Konarev, S. S. Khasanov, A. Otsuka, G. Saito and R. N. Lyubovskaya, *Inorg. Chem.*, 2007, **46**, 2261.
25 D. V. Konarev, S. S. Khasanov, Yu. L. Slovokhotov, G. Saito and R. N. Lyubovskaya, *CrystEngComm*, 2008, **10**, 48.
26 D. V. Konarev, S. S. Khasanov, A. Otsuka, G. Saito and R. N. Lyubovskaya, *CrystEngComm*, 2009, **11**, 811.
27 D. V. Konarev, S. S. Khasanov, E. I. Yudanova and R. N. Lyubovskaya, *Eur. J. Inorg. Chem.*, 2011, 816.
28 G. M. Sheldrick, *SHELX97*, University of Göttingen, Germany, 1997.